Alternative Modes of Bonding of C_4F_8 Units in Mononuclear and Binuclear Iron Carbonyl Complexes

Liping Huang,[a] Jing Li,[a] Guoliang Li,*[a,b] Yaoming Xie,[b] R. Bruce King,*[b] and Henry F. Schaefer[b]

[a]*Key Laboratory of Theoretical Chemistry of the Environment, Ministry of Education; Center for Computational Quantum Chemistry, School of Chemistry and Environment, South China Normal University, Guangzhou 510006, P. R. China*

[b]*Department of Chemistry and Center for Computational Quantum Chemistry, University of Georgia, Athens, Georgia 30602, USA*

e-mails: rbking@chem.uga.edu and glli@scnu.edu.cn

ABSTRACT

Density functional theory studies show that the lowest energy $C_4F_8Fe(CO)_4$ structure is not the very stable experimentally known ferracyclopentane isomer $(CF_2CF_2CF_2CF_2)Fe(CO)_4$ obtained from $Fe(CO)_{12}$ and tetrafluoroethylene. Instead isomeric (perfluoroolefin)$Fe(CO)_4$ structures derived from perfluoro-2-butene, perfluoro-1-butene, and perfluoro-2-methylpropene are significantly lower energy structures by up to ~17 kcal/mol. However, the activation energies for the required fluorine shifts from one carbon to an adjacent carbon atom to form these (perfluoroolefin)$Fe(CO)_4$ complexes from tetrafluoroethylene are very high (e.g., ~70 kcal/mol). Therefore the ferracyclopentane isomer $(CF_2CF_2CF_2CF_2)Fe(CO)_4$, which does not require a fluorine shift to form from $Fe_3(CO)_{12}$ and tetrafluoroethylene, is the kinetically favored product. The lowest energy structures of the binuclear $(C_4F_8)_2Fe_2(CO)_n$ ($n = 7, 6$) derivatives have bridging perfluorocarbene ligands and terminal perfluoroolefin ligands.

Keywords: Octafluorobutene, Metallacycles, Fluorinated Carbenes, Olefin Complexes, Iron carbonyls, Density functional theory

1. Introduction

The ability of perfluorination to stabilize transition metal alkyl derivatives was first recognized in the early 1960s shortly after the first syntheses of fluorocarbon transition metal derivatives using reagents such as perfluoroalkyl iodides and tetrafluoroethylene to introduce the fluorocarbon moiety. The most dramatic early example of such stabilization was found in the alkylcobalt carbonyl derivatives $CX_3Co(CO)_4$ (X = H, F). Thus $CH_3Co(CO)_4$ decomposes at –40°C whereas its perfluorinated analogue $CF_3Co(CO)_4$ is a yellow liquid that can be distilled at atmospheric pressure around 100°C.[1,2]

The ability of perfluorination to stabilize transition metal alkyls can be related to the high electronegativity of perfluoroalkyl groups. This can lead to $d\pi \rightarrow \sigma^*$ back donation of electrons from filled transition metal d orbitals into C–F antibonding orbitals on the α-carbon atom adjacent to the transition metal (Figure 1). This is closely related to the better known[3] $d\pi \rightarrow p\pi^*$ back donation into C–O antibonding orbitals in metal carbonyls. The stabilization of metal-carbon bonds to fluorocarbon ligands by such back donation has led to the extensive development of fluorocarbon transition metal chemistry.[4,5,6]

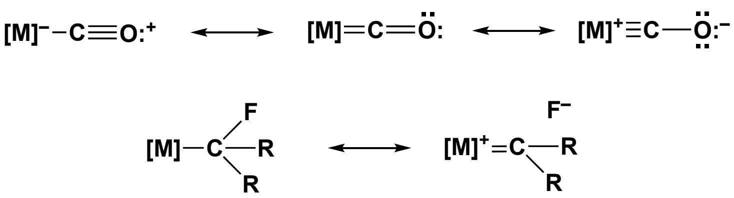

Figure 1. Resonance structures generated by back donation of electrons from filled metal d orbitals into antibonding orbitals of carbonyl and perfluoroalkyl ligands showing the "no-bond" resonance labilizing the fluorine atoms in the latter systems.

The $d\pi \rightarrow p\pi^*$ back donation in metal carbonyl chemistry into antibonding orbitals of the C-O multiple bonds of the carbonyl ligands reduces their effective bond order as typically reflected in lowering of the ν(CO) frequencies upon metal complexation of free carbon monoxide (Figure 1). However, since the C≡O bond in free carbon monoxide is already a formal triple bond, such lowering of the effective bond order is not normally sufficient to break the C-O bond. The reduction of the C–F bond order through analogous $d\pi \rightarrow \sigma^*$ back donation into antibonding C-F orbitals similarly reduces the effective C–F bond order. This leads formally to a type of "no bond" resonance involving polarized canonical structures with zero bond order of the C-F "bonds" to the α-carbon atom adjacent to the transition metal. This weakening of these C–F bonds to the α-carbon atom of fluoroalkyl transition metal derivatives activates such fluorine atoms thereby making them susceptible for migration to other atoms.[7]

Fluorine migration from α-carbon atoms in perfluoroalkyl transition metal derivatives was first observed in the study of $Co_2(CO)_8$ with tetrafluoroethylene (Figure 2).[8,9] Under mild conditions the initial product is a yellow solid formulated as $(OC)_4CoCF_2CF_2Co(CO)_4$ in which each tetrafluoroethylene carbon atom forms a σ-bond to the cobalt atom of a $Co(CO)_4$ unit. This initial product is a binuclear relative of $CF_3Co(CO)_4$ and has a similar yellow color. However, this yellow octacarbonyl reversibly loses CO under mild conditions to give the red heptacarbonyl $(\mu\text{-}CF_3CF)Co_2(CO)_6(\mu\text{-}CO)$ in which fluorine migration has occurred to convert the bridging CF_2CF_2 unit in the initial yellow product to a trifluoromethyl carbene ligand CF_3CF. This loss of a carbonyl group from the initial $(OC)_4CF_2CF_2Co(CO)_4$ concurrently results in the formation of a direct Co–Co bond that is bridged by the CF_3CF ligand. This trifluoromethyl carbene complex is relatively stable. However, upon reaction with excess $Co_2(CO)_8$ the lone fluorine atom bonded to the α-carbon atom is lost leading to the dark purple cluster $CF_3CCo_3(CO)_9$. Presumably the fluorine on the α-carbon atom in $(\mu\text{-}CF_3CF)Co_2(CO)_6(\mu\text{-}CO)$ migrates from carbon to cobalt. This would be expected to lead ultimately to CoF_2, owing to the instability of cobalt carbonyl fluorides towards loss of the carbonyl groups.

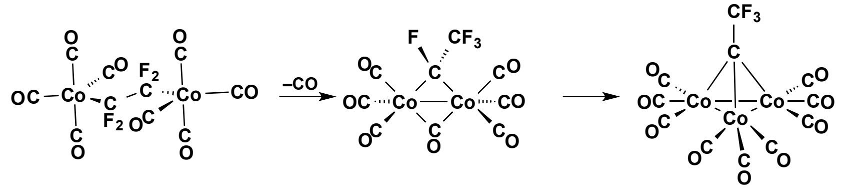

$(OC)_4CoCF_2CF_2Co(CO)_4$ $(\mu\text{-}CF_3CF)Co_2(CO)_6(\mu\text{-}CO)$ $CF_3CCo_3(CO)_9$

Figure 2. The cobalt carbonyl derivatives obtained from reactions of $Co_2(CO)_8$ with tetrafluoroethylene.

The reaction of tetrafluoroethylene with iron carbonyls was found in very early work of Wilkinson et al. to follow a different course.[10,11,12] Thus reaction of $Fe_3(CO)_{12}$ with tetrafluoroethylene under more vigorous conditions than required for the formation of $CF_3CCo_3(CO)_9$ from tetrafluoroethylene and $Co_2(CO)_8$ results in dimerization of C_2F_4 on the iron site to give the perfluorinated ferracyclopentane metallacycle $C_4F_8Fe(CO)_4$ (Figure 3). No evidence was observed for a single fluorine shift to give the isomeric fluorinated carbene complexes $(CF_3)(CF_3CF_2)C{=}Fe(CO)_4$ or $(CF_3CF_2CF_2)C(F){=}Fe(CO)_4$ or for a double fluorine shift to give the isomeric perfluoroolefin complexes $(\eta^2\text{-}CF_3CF{=}CFCF_3)Fe(CO)_4$ or $(\eta^2\text{-}CF_3CF_2CF{=}CF_2)Fe(CO)_4$ (Figure 3), despite the severity of the reaction conditions.

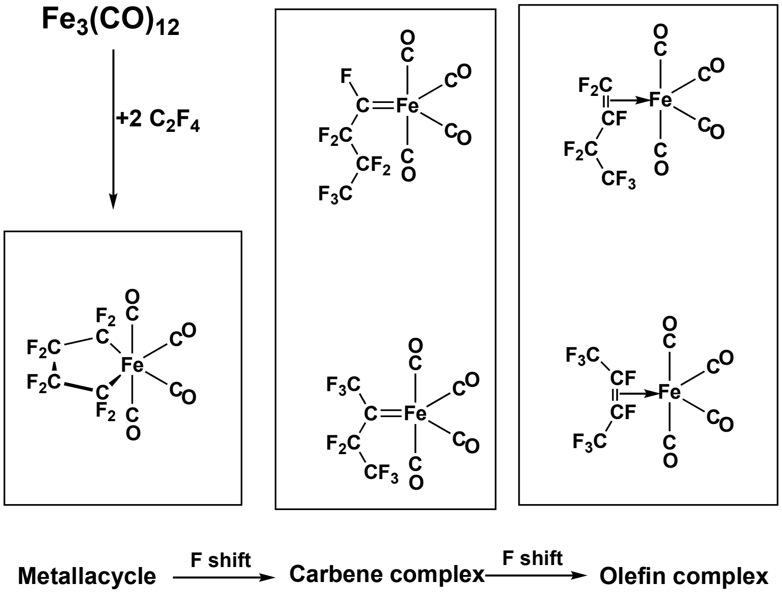

Figure 3. Isomeric perfluorinated carbene and perfluoroolefin iron carbonyl complexes derived from the known perfluorinated ferracyclopentane $C_4F_8Fe(CO)_4$ by fluorine migration. The fluorine-shift reactions are hypothetical and have not been observed.

The central iron atom in the metallacycle $C_4F_8Fe(CO)_4$ is octahedrally coordinated to six strong back bonding ligands, namely the four carbonyl groups and the two terminal CF_2 groups forming the C_4F_8 chain within the ferracyclopentane ring. In this way this iron atom resembles the central chromium atom in $Cr(CO)_6$, which is octahedrally coordinated to six carbonyl groups. Both $C_4F_8Fe(CO)_4$ and $Cr(CO)_6$ are volatile air-stable white solids, consistent with the favorable 18-electron configuration of the central metal atom. Because of the similarity of the mononuclear derivatives $C_4F_8Fe(CO)_4$ and $Cr(CO)_6$, the corresponding binuclear derivatives $(C_4F_8)_2Fe_2(CO)_n$ (n = 7, 6) and $Cr_2(CO)_{n+4}$ might be expected to be similar.

The binary binuclear chromium carbonyls $Cr_2(CO)_{11}$ and $Cr_2(CO)_{10}$ are not known experimentally as stable species. This is consistent with theoretical studies[13,14] showing them to be disfavored relative to dissociation into mononuclear derivatives including the very stable $Cr(CO)_6$. Thus the lowest energy $Cr_2(CO)_{11}$ structure has a relatively long Cr–Cr single bond (3.15 Å) consistent with its predicted exothermic dissociation into $Cr(CO)_6$ + $Cr(CO)_5$.[13] Low-energy structures for the formally unsaturated $Cr_2(CO)_{10}$ include a singlet with two four-electron donor bridging η^2-μ-CO groups and no formal metal-metal bonding and a triplet state with exclusively terminal CO groups and a formal Cr=Cr double bond similar to the O=O bond in triplet O_2.[14]

We now report the use of density functional theory to explore the geometry and energetics of the $C_4F_8Fe(CO)_4$, $(C_4F_8)_2Fe_2(CO)_7$, and $(C_4F_8)_2Fe_2(CO)_6$ systems analogous to the $Cr(CO)_6$, $Cr_2(CO)_{11}$, and $Cr_2(CO)_{10}$ systems. The experimental ferracyclopentane structure for $C_4F_8Fe(CO)_4$ obtained from $Fe_3(CO)_{12}$ and tetrafluoroethylene is found to be a higher energy structure than isomeric perfluorobutene structures requiring fluorine migration for their formation. However, the initial step of the required fluorine migration step is found to have a high activation energy around ~70 kcal/mol. thereby accounting for the experimental observation of the kinetically favored ferracyclopentane isomer. In the binuclear systems $(C_4F_8)_2Fe_2(CO)_n$ (n = 7, 6) fluorine migration is predicted to occur to give isomers with bridging perfluorocarbene ligands rather than perfluoroolefin isomers as the lowest energy structures. This suggests that the Fe–Fe bond in the binuclear derivatives plays a critical role by providing a bridging site for a perfluorocarbene ligand generated by fluorine migration from a perfluorinated ferracyclopentane ring.

2. Theoretical Methods

Electron correlation effects have been included to some degree in density functional theory (DFT) methods, which have evolved as a practical and effective computational tool, especially for organometallic compounds.[15-21] In this research, the newer generation M06-L method was employed. The M06-L method using a meta-GGA functional proposed by Zhao and Truhlar[22] was found to be suitable for applications in transition metal chemistry.[23,24] The basis sets used herein were the correlation-consistent polarized valence triple-ζ (cc-pVTZ) variety. The cc-pVTZ basis sets for carbon, oxygen, and fluorine atoms are given by Dunning,[25] while those for iron come from Balabanov and Peterson.[26] Other popular DFT methods, such as B3LYP,[27,28] BP86,[29,30] and BPW91,[29,31] were found to be useful for bare iron clusters and those interacting with CO molecules.[32,33] In the present study, we have also tested these functionals for the $C_4F_8Fe(CO)_4$ system (Table **S1** in the Supporting Information). We found the results using these other functionals to be similar to those from the M06-L method.

The $C_4F_8Fe(CO)_4$, $(C_4F_8)_2Fe_2(CO)_7$, and $(C_4F_8)_2Fe_2(CO)_6$ structures were fully optimized using the M06-L/cc-pVTZ method. Both singlet and triplet spin states were considered. However, all of the triplet structures were found to have higher energies than the corresponding singlet structures and thus are not discussed in this paper. Harmonic vibrational frequency analyses were also carried out at the same level of theory. All the computations were carried out with the Gaussian 09 program,[34] with an ultrafine grid (99, 590) for numerical integration. The convergence criterion for the SCF energy was

10^{-8} E_h, and a tight (10^{-5} a.u.) convergence criterion was for optimization. A given $(C_4F_8)_mFe_m(CO)_n$ structure is designated as **mn-dS** where **m** is the number of iron atoms and C_4F_8 groups, **n** is the number of CO groups, **d** orders the structures according to their relative energies, and **S** refers to the singlet spin state. Thus the lowest energy singlet $(C_4F_8)_2Fe_2(CO)_7$ structure is designated **27-1S**. The relative energies (ΔE) in the text are based on the total electronic energies without ZPE (zero point energy) corrections. The relative energies with ZPE correction are shown in Table **S2** in the Supporting Information.

3. Results and Discussion

3.1 Mononuclear derivatives

The C_4F_8 ligand can exhibit nine different types of isomeric structures, i.e. CF_3-CF_2-CF=CF_2 (perfluoro-1-butene), CF_3-CF=CF-CF_3 (perfluoro-2-butene), CF_3-C(CF_3)=CF_2 (perfluoro-2-methylpropene), -CF_2-CF_2-CF_2-CF_2- (perfluoro-tetramethylene), -CF(CF_3)-CF_2-CF_2- (perfluoro-1-methyltrimethylene), -CF_2-CF(CF_3)-CF_2- (perfluoro-2-methyltrimethylene), CF_3-CF_2-CF_2-CF= (perfluorobutylidene), CF_3-CF_2-C(CF_3)= (perfluoro-1-methylpropylidene), and CF_3-CF(CF_3)-CF= (perfluoro-2-methylpropylidene). The singlet CF_3-C(CF_3)=CF_2 structure has the lowest energy. The relative energies of the structures with CF_3-CF=CF-CF_3 (singlet), CF_3-CF_2-CF=CF_2 (singlet), CF_3-CF(CF_3)-CF= (singlet), CF_3-CF_2-C(CF_3)= (triplet), CF_3-CF_2-CF_2-CF= (singlet), -CF(CF_3)-CF_2-CF_2- (triplet), -CF_2-CF(CF_3)-CF_2- (triplet), and -CF_2-CF_2-CF_2-CF_2- (triplet) units are 12.3, 19.2, 70.3, 71.1, 77.8, 78.2, 80.5, and 86.8 kcal/mol, respectively, at the M06-L/cc-pVTZ level of theory. Coordinating these isomeric C_4F_8 ligands to an $Fe(CO)_4$ unit leads to nine different kinds of $C_4F_8Fe(CO)_4$ structures, designated as **14-1S** to **14-9S** in Figure 4.

The three perfluoroolefin complex structures **14-1S**, **14-2S**, and **14-3S** have the lowest energies. Among these three isomers, the perfluoro-2-methylpropene complex [η^2-CF_3-C(CF_3)=CF_2]$Fe(CO)_4$ (**14-1S**) has the lowest energy. The perfluoro-2-butene complex (η^2-CF_3-CF=CF-CF_3)$Fe(CO)_4$ (**14-2S**) and the perfluoro-1-butene complex (η^2-CF_3-CF_2-CF=CF_2)$Fe(CO)_4$ (**14-3S**) lie 4.7 and 14.8 kcal/mol, respectively, in energy above **14-1S**. In **14-1S**, **14-2S** and **14-3S**, the C=C double bond lengths are ~1.44 Å, which are ~0.07 Å shorter than the C-C bond lengths. Next in energy comes the experimentally known perfluorinated metallacyclopentane complex (η^2-CF_2-CF_2-CF_2-CF_2)$Fe(CO)_4$ (**14-4S**), lying 16.8 kcal/mol above **14-1S**. The perfluorinated ferracyclobutane structures [η^2-CF_2-CF_2-CF(CF_3)-]$Fe(CO)_4$ (**14-5S**) and

[η^2-CF_2-$CF(CF_3)$-CF_2-]$Fe(CO)_4$ (**14-6S**), lie 17.2 and 21.1 kcal/mol, respectively, in energy above **14-1S**. The three perfluorinated carbene complex structures, namely the perfluoro-2-methylpropylidene complex CF_3-$CF(CF_3)$-$C(F)$=$Fe(CO)_4$ (**14-7S**), the perfluoro-1-methylpropylidene complex CF_3-CF_2-$C(CF_3)$=$Fe(CO)_4$ (**14-8S**) and the perfluorobutylidene complex CF_3-CF_2-CF_2-$C(F)$=$Fe(CO)_4$, have the highest energies, at more than 22 kcal/mol above **14-1S**. The Fe-C bond distances in the η^2-C_4F_8 structures (**14-1S** to **14-6S**) range from 2.007 to 2.085 Å, corresponding to Fe-C single bonds. However, the Fe=C bond distances in all of the carbene η^1-C_4F_8 structures (**14-7S** to **14-9S**) are ~0.2 Å shorter than the Fe-C single bond distances, ranging from 1.832 to 1.860 Å and thus can correspond to Fe=C double bonds. Thus, in all of the $C_4F_8Fe(CO)_4$ complexes the C_4F_8 ligands are two-electron donors, thereby giving each iron atom in these structures the favored 18-electron configuration.

The very stable experimentally known metallacyclopentane structure **14-4S** is the only $C_4F_8Fe(CO)_4$ isomer that can be formed from tetrafluoroethylene and iron carbonyls without fluorine migration. However, the three perfluoroolefin complexes **14-1S**, **14-2S**, and **14-3S** all lie at significantly lower energies than **14-4S**. Thus **14-4S** is the kinetically favored product from $Fe_3(CO)_{12}$ and tetrafluoroethylene whereas the lowest energy isomer with a straight C_4 chain, namely **14-2S**, lies ~12 kcal/mol in energy below **14-4S**. However, investigation of the relevant portion of the potential energy surface of the $C_4F_8Fe(CO)_4$ system (Figure 5) predicts a high activation energy of 70.5 kcal/mol (= 87.3 – 16.8 kcal/mol) for the first fluorine shift in the conversion of **14-4S** to **14-2S**. This can account for the formation of the very stable ferracyclopentane **14-4S** as the kinetic product from $Fe_3(CO)_{12}$ and tetrafluoroethylene. The $C_4F_8Fe(CO)_4$ global minimum **14-1S**, lying 4.7 kcal/mol in energy below **14-2S**, has a branched $C_3(C)$ chain and thus requires rupture of a C–C bond for formation from **14-2S**. In view of the kinetic stability of C–C bonds, it is not unreasonable to suppose that conversion of a straight C_4 chain, such as that in **14-2S**, to a branched $C_3(C)$ chain, such as that in **14-1S**, would require a significantly higher activation energy than rupture of a C–F bond in the conversion of **14-4S** to **14-2S**.

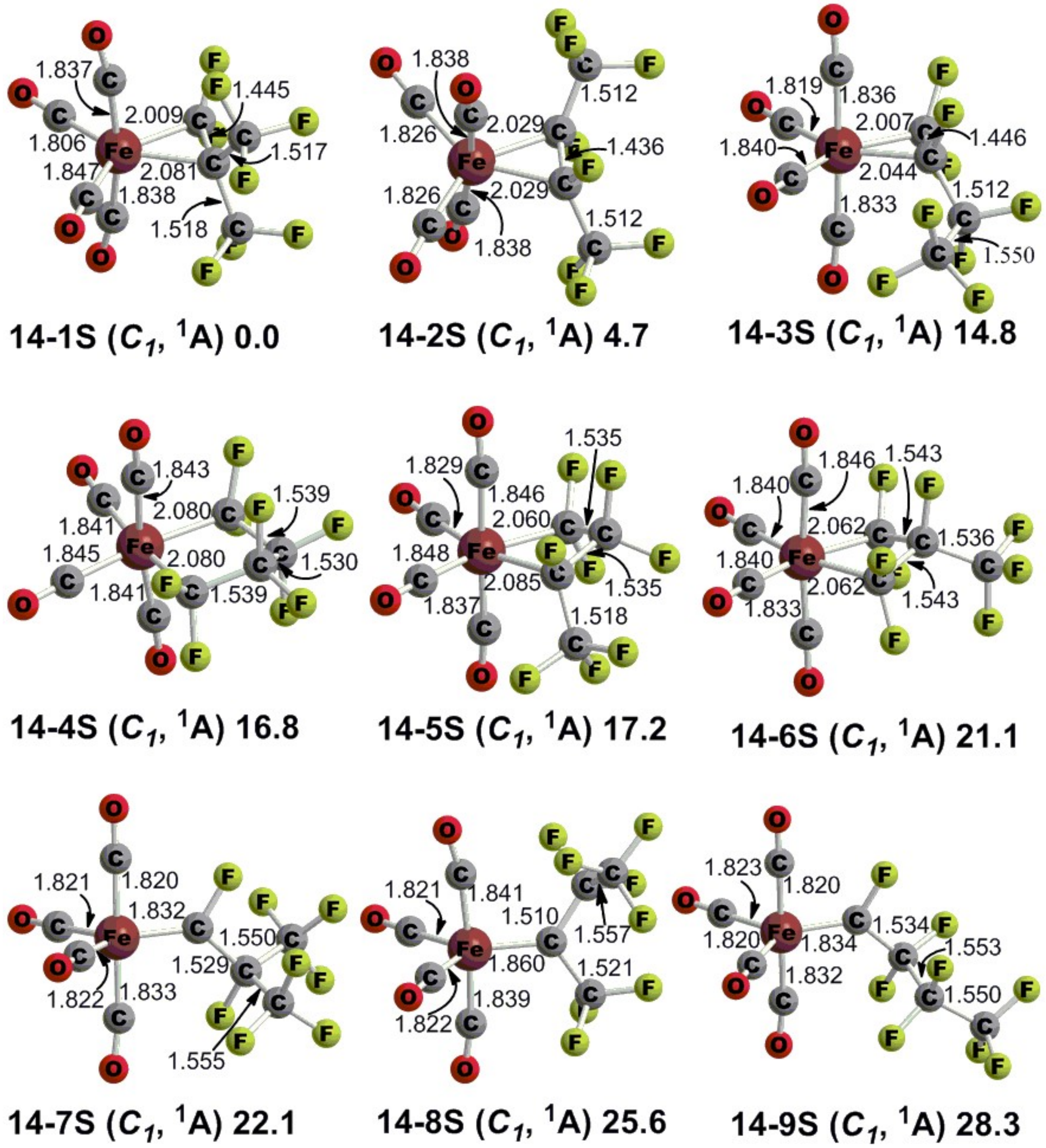

14-1S (C_1, ^{1}A) 0.0 **14-2S** (C_1, ^{1}A) 4.7 **14-3S** (C_1, ^{1}A) 14.8

14-4S (C_1, ^{1}A) 16.8 **14-5S** (C_1, ^{1}A) 17.2 **14-6S** (C_1, ^{1}A) 21.1

14-7S (C_1, ^{1}A) 22.1 **14-8S** (C_1, ^{1}A) 25.6 **14-9S** (C_1, ^{1}A) 28.3

Figure 4. Optimized $C_4F_8Fe(CO)_4$ structures. In Figures 4 to 9, the bond distances (in Å) and relative energies (in kcal/mol, under each structure) were obtained at the M06-L/cc-pVTZ level of theory.

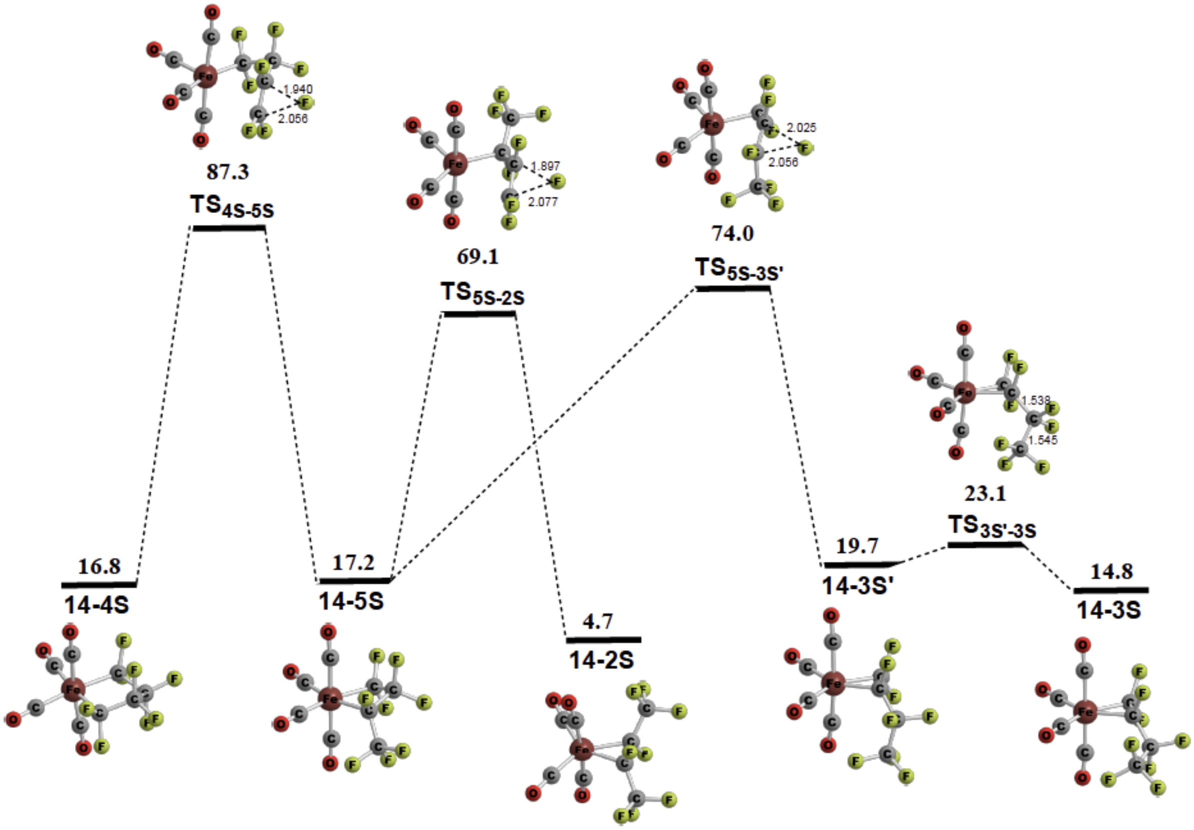

Figure 5. Energy profile for the conversion of the kinetically favored metallacyclopentane product **14-4S** from $Fe_3(CO)_{12}$ and tetrafluoroethylene to the lowest energy isomer with a C_4 straight chain, namely **14-2S**. Each transition state (TS) was optimized starting from a reasonable initial structure based on the two minima it connects. The optimized TS structures were confirmed with the intrinsic reaction coordinate (IRC) analysis.[35,36,37]

3.2 Binuclear derivatives

3.2.1 $(C_4F_8)_2Fe_2(CO)_7$

Twenty-three singlet $(C_4F_8)_2Fe_2(CO)_7$ structures are found within ~20 kcal/mol of the lowest energy structure **27-1S**. These 23 structures can be divided into three types: singly C_4F_8-bridged structures, triply C_4F_8- and CO-bridged structures and singly CO-bridged structures. These structures are discussed below according to their structure type.

Singly C_4F_8-bridged structures. Ten low-energy singly C_4F_8-bridged $(C_4F_8)_2Fe_2(CO)_7$ structures are found with one C_4F_8 group bonded to two iron atoms as a bridge and the other C_4F_8 group coordinated with only one iron atom as a terminal group, namely **27-1S**, **27-4S**, **27-6S**, **27-10S**, **27-12S**, **27-14S**, **27-15S**, **27-17S**, **27-21S**, and **27-22S** (Figure 6). In these singly-C_4F_8 bridged $Fe_2(\mu\text{-}C_4F_8)(C_4F_8)(CO)_7$ structures, the bridging C_4F_8 group is either a perfluoro-1-methylpropylidene, a perfluoro-2-methylpropylidene, or a perfluorobutylidene group, while the terminal C_4F_8 group is a perfluoro-2-methylpropene, a perfluoro-2-butene, or a perfluoro-1-butene ligand. Thus, bridging C_4F_8 groups prefer carbene structures while terminal C_4F_8 groups prefer olefin structures. The lowest energy $(C_4F_8)_2Fe_2(CO)_7$ structure **27-1S** has a bridging perfluoro-1-methylpropylidene and a terminal perfluoro-2-methylpropene group. Structure **27-4S**, lying only 2.4 kcal/mol in energy above **27-1S**, also has a bridging perfluoro-1-methylpropylidene group, but its terminal C_4F_8 ligand is a perfluoro-2-butene group. Replacing the bridging perfluoro-1-methylpropylidene group in **27-1S** with a perfluoro-2-methylpropylidene or a perfluorobutylidene group, gives **27-6S** or **27-10S**, respectively, lying 5.3 and 5.9 kcal/mol, respectively, in energy above **27-1S**. Similarly, replacing the bridging perfluoro-1-methylpropylidene group in **27-4S** with a perfluoro-2-methylpropylidene or a perfluorobutylidene group gives **27-12S** or **27-14S**, lying 5.5 and 6.8 kcal/mol in energy, respectively, above **27-4S**. Structures **27-15S**, **27-21S**, and **27-22S**, lying 12.3, 19.4, and 19.9 kcal/mol, respectively, in energy above **27-1S**, all have terminal perfluorobutylidene groups and differ only by different bridging C_4F_8 groups. Structure **27-17S**, with a terminal perfluoro-2-methylpropylidene and a bridging perfluoro-1-methylpropylidene group, lying 14.3 kcal/mol in energy above **27-1S**, is the only $Fe_2(\mu\text{-}C_4F_8)(C_4F_8)(CO)_7$ structure in which the terminal C_4F_8 ligand is not an olefin. The Fe–Fe distances of 2.60 to 2.69 Å in these ten singly C_4F_8-bridged $Fe_2(\mu\text{-}C_4F_8)(C_4F_8)(CO)_7$ structures suggest formal single bonds. Considering all of the C_4F_8 ligands as two-electron donors give each iron atom in these structures the favored 18-electron configuration.

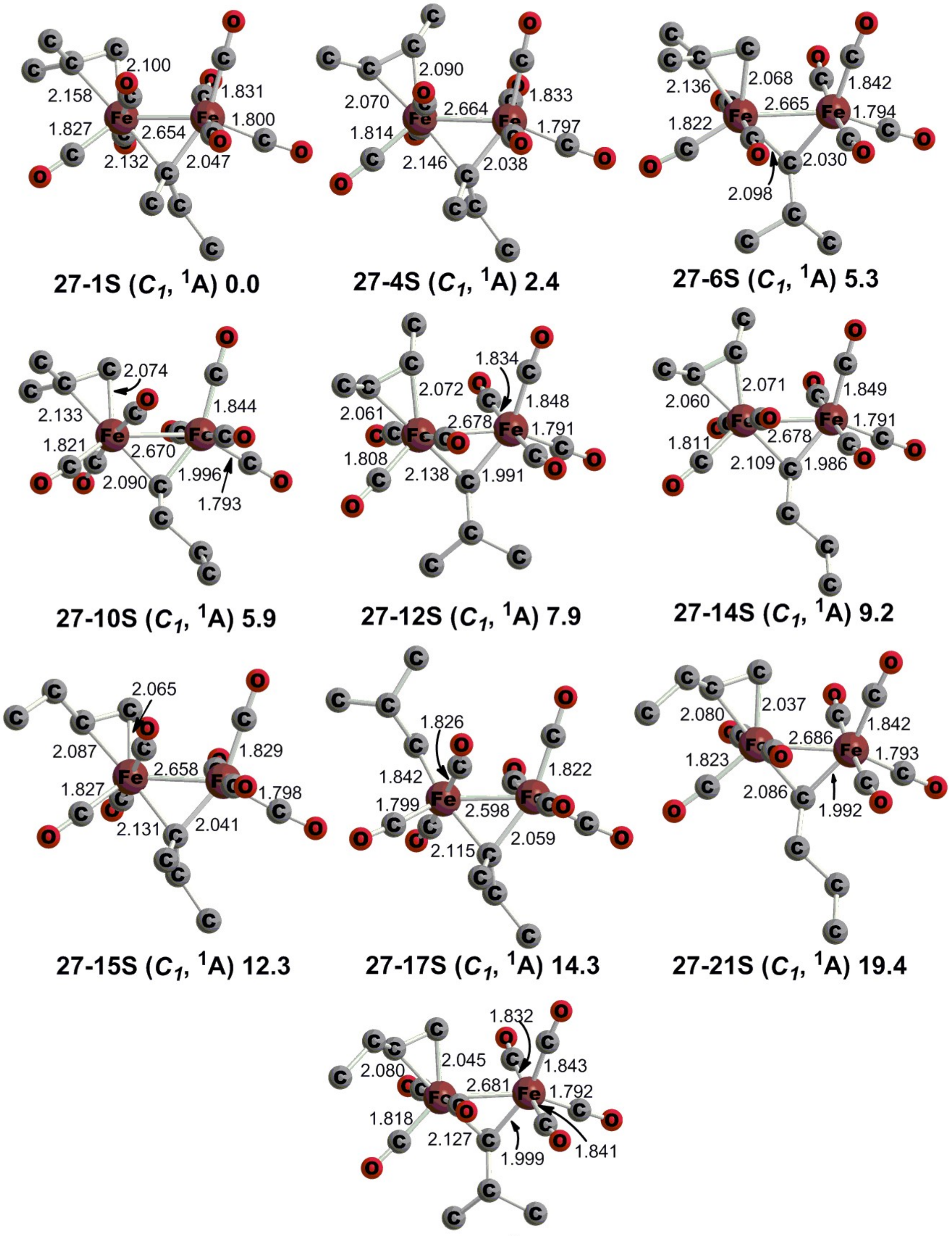

27-1S (C_1, ^{1}A) 0.0 **27-4S (C_1, ^{1}A) 2.4** **27-6S (C_1, ^{1}A) 5.3**

27-10S (C_1, ^{1}A) 5.9 **27-12S (C_1, ^{1}A) 7.9** **27-14S (C_1, ^{1}A) 9.2**

27-15S (C_1, ^{1}A) 12.3 **27-17S (C_1, ^{1}A) 14.3** **27-21S (C_1, ^{1}A) 19.4**

27-22S (C_1, ^{1}A) 19.9

Figure 6. The ten low-energy singly C_4F_8-bridged $(C_4F_8)_2Fe_2(CO)_7$ structures, with all fluorine atoms omitted for the sake of clarity.

Triply C_4F_8- and CO-bridged structures. Nine low-energy triply bridged $(C_4F_8)_2Fe_2(CO)_7$ structures are found with two bridging C_4F_8 groups and one bridging CO group connecting the two iron atoms, i.e. **27-2S**, **27-5S**, **27-7S**, **27-8S**, **27-9S**, **27-11S**, **27-19S**, **27-20S**, and **27-23S** (Figure 7). As with the singly bridged structures discussed above, bridging C_4F_8 groups prefer carbene structures, namely perfluoro-1-methylpropylidene, perfluoro-2-methylpropylidene, or perfluorobutylidene. The six low-energy triply bridged $Fe_2(\mu\text{-}C_4F_8)_2(\mu\text{-}CO)(CO)_6$ structures **27-2S**, **27-5S**, **27-7S**, **27-8S**, **27-9S** and **27-11S**, with two bridging C_4F_8 carbene groups and one bridging carbonyl group, exemplify different ways of combining the three types of C_4F_8 perfluorocarbene bridges. Thus, **27-2S** has one perfluoro-1-methylpropylidene bridge and perfluorobutylidene bridge. Structure **27-5S** has one perfluoro-1-methylpropylidene bridge and one perfluoro-2-methylpropylidene bridge. Structure **27-7S** has two bridging perfluoro-2-methylpropylidene groups. Structure **27-8S** has one perfluorobutylidene bridge and one perfluoro-2-methylpropylidene bridge. Structure **27-9S** has two bridging perfluoro-1-methylpropylidene groups whereas structure **27-11S** has two bridging perfluorobutylidene groups. Energetically, structures **27-2S**, **27-5S**, **27-7S**, **27-8S**, **27-9S** and **27-11S** lie 1.5, 3.0, 5.4, 5.5, 5.9, and 6.1 kcal/mol, respectively, above **27-1S**. The Fe–Fe distances in **27-2S**, **27-5S**, **27-7S**, **27-8S**, **27-9S** and **27-11S** range from 2.46 to 2.49 Å, which is ~0.20 Å shorter than the Fe–Fe distances in the singly C_4F_8 bridged $Fe_2(\mu\text{-}C_4F_8)(C_4F_8)(CO)_7$ structures discussed above. This Fe–Fe bond shortening effect in these six structures appears to be a consequence of the three bridging groups. Interpreting the Fe–Fe bonds in these six structures are formal single bonds gives each iron atom the favored 18-electron configuration.

We also found some $Fe_2(\mu\text{-}C_4F_8)_2(\mu\text{-}CO)(CO)_6$ triply bridged structures in which one bridging C_4F_8 group is not a carbene but an olefin. Thus the three $Fe_2(\mu\text{-}C_4F_8)_2(\mu\text{-}CO)(CO)_6$ structures **27-19S**, **27-20S**, and **27-23S**, each have only one bridging carbene C_4F_8 group, with the other bridging C_4F_8 group being an olefin. However, these three structures are much less energetically favorable, lying at least 18 kcal/mol in energy above **27-1S**.

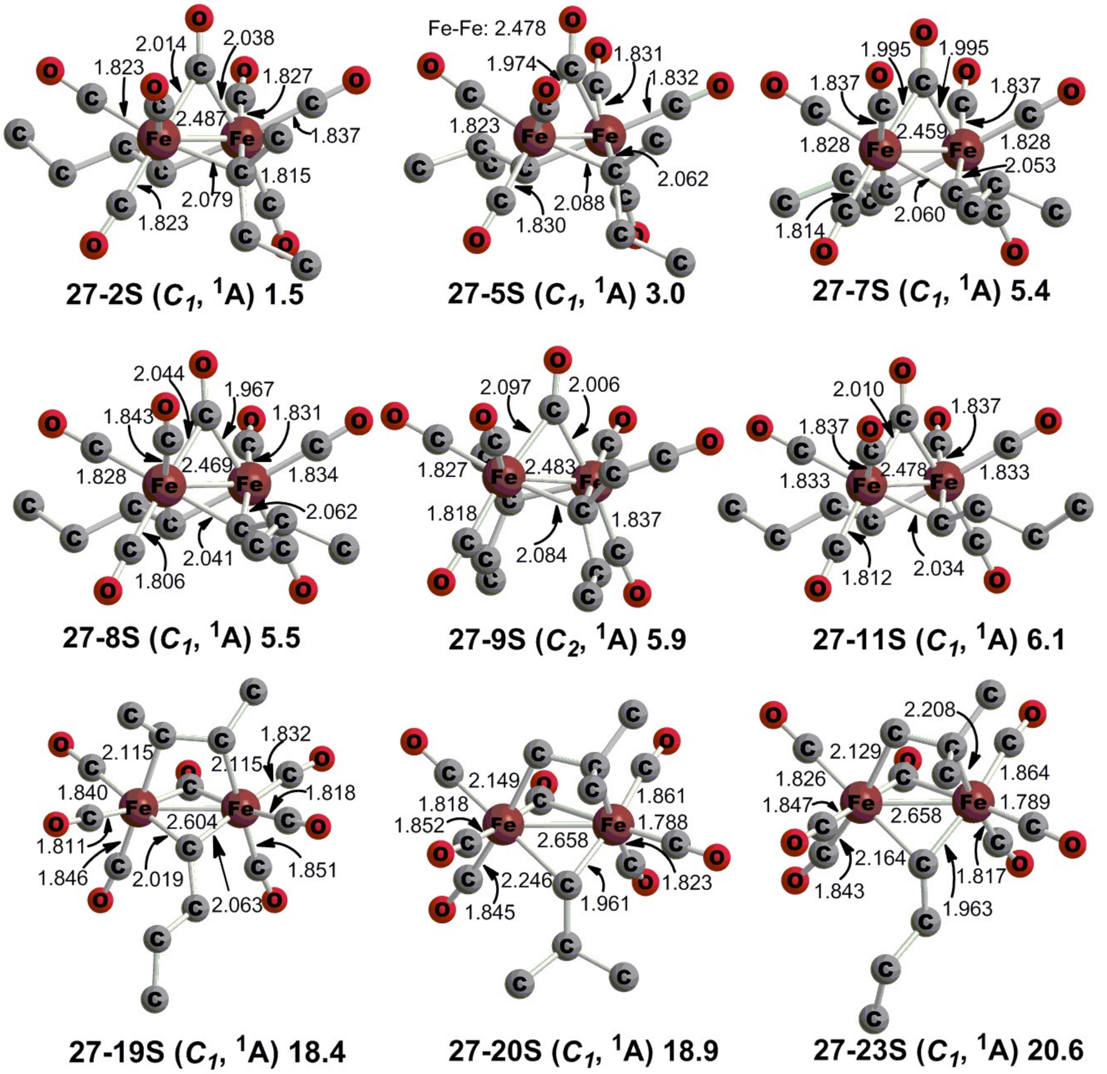

27-2S (C_1, ^{1}A) 1.5
27-5S (C_1, ^{1}A) 3.0
27-7S (C_1, ^{1}A) 5.4
27-8S (C_1, ^{1}A) 5.5
27-9S (C_2, ^{1}A) 5.9
27-11S (C_1, ^{1}A) 6.1
27-19S (C_1, ^{1}A) 18.4
27-20S (C_1, ^{1}A) 18.9
27-23S (C_1, ^{1}A) 20.6

Figure 7. Optimized low-energy triply C_4F_8- and CO-bridged $(C_4F_8)_2Fe_2(CO)_7$ structures ,with all fluorine atoms omitted for the sake of clarity.

Singly CO-bridged structures. Four low-energy singly CO-bridged $(C_4F_8)_2Fe_2(CO)_7$ structures are found, namely **27-3S**, **27-13S**, **27-16S**, and **27-18S**, in which all of the terminal C_4F_8 groups are the perfluoroolefins perfluoro-2-methylpropene, perfluoro-2-butene, or perfluoro-1-butene (Figure 8). This again indicates the preference of terminal C_4F_8 groups for olefin structures. The lowest-energy singly-CO bridged $Fe_2(\mu\text{-}CO)(C_4F_8)_2(CO)_6$ structure **27-3S**, lying only 1.7 kcal/mol in energy above **27-1S**, has two terminal perfluoro-2-methylpropene ligands. Replacing one terminal perfluoro-2-methylpropene ligand in **27-3S** with a perfluoro-2-butene ligand and with a perfluoro-1-butene ligand gives **27-13S** and **27-18S**, respectively, lying 6.5 and 13.5 kcal/mol, respectively, in energy above **27-3S**. Structure **27-16S**, lying 13.3 kcal/mol in energy above **27-1S**, has two terminal perfluoro-2-butene ligands. The Fe–Fe distances of 2.80 to 2.87 Å in these four singly CO-bridged $Fe_2(\mu\text{-}CO)(C_4F_8)_2(CO)_6$ structures are ~0.20 Å longer than those in the singly C_4F_8-bridged $Fe_2(\mu\text{-}C_4F_8)(C_4F_8)(CO)_7$ structures discussed above. However, they still suggest formal single bonds, thereby giving each iron atom in the favored 18-electron configuration.

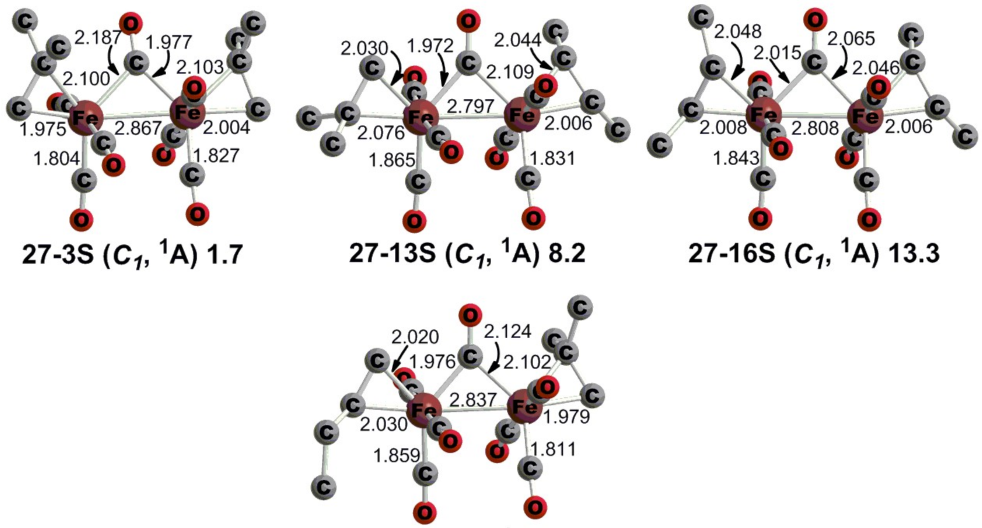

27-3S (C_1, ^1A) 1.7 **27-13S** (C_1, ^1A) 8.2 **27-16S** (C_1, ^1A) 13.3

27-18S (C_1, ^1A) 15.2

Figure 8. Optimized low-energy singly CO-bridged $(C_4F_8)_2Fe_2(CO)_7$ structures, with all fluorine atoms omitted for the sake of clarity.

3.2.2 $(C_4F_8)_2Fe_2(CO)_6$

Removing a CO group from the $(C_4F_8)_2Fe_2(CO)_7$ structures above leads to a variety of $(C_4F_8)_2Fe_2(CO)_6$ structures. Since many such $(C_4F_8)_2Fe_2(CO)_6$ structures are very similar, only the lowest energy $(C_4F_8)_2Fe_2(CO)_6$ structure derived from each $(C_4F_8)_2Fe_2(CO)_7$ structure is discussed. Eleven $(C_4F_8)_2Fe_2(CO)_6$ structures, namely **26-1S** to **26-11S**, are found within ~20 kcal/mol of the lowest energy structure **26-1S** (Figure 9). The dissociation energy for the loss of a CO group from the lowest energy $(C_4F_8)_2Fe_2(CO)_7$ structure **27-1S** to give the lowest energy $(C_4F_8)_2Fe_2(CO)_6$ structure **26-1S** is 13.1 kcal/mol.

All of these $(C_4F_8)_2Fe_2(CO)_6$ structures are singlet spin state structures. Similar to the $(C_4F_8)_2Fe_2(CO)_7$ structures, these $(C_4F_8)_2Fe_2(CO)_6$ structures can be divided into three types: singly C_4F_8-bridged structures, triply C_4F_8- and CO-bridged structures, and singly CO-bridged structures.

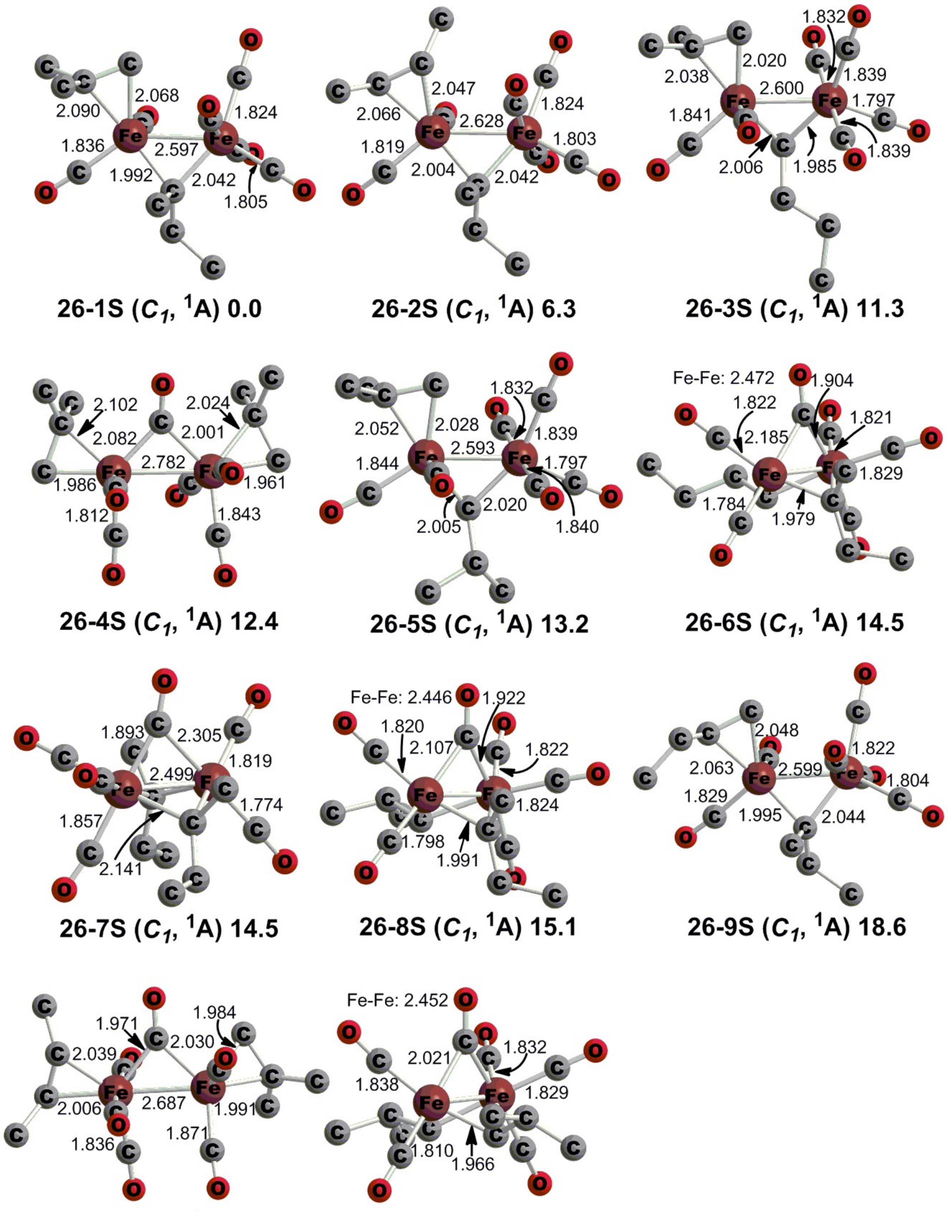

26-1S (*C_1*, ^{1}A) 0.0 **26-2S** (*C_1*, ^{1}A) 6.3 **26-3S** (*C_1*, ^{1}A) 11.3

26-4S (*C_1*, ^{1}A) 12.4 **26-5S** (*C_1*, ^{1}A) 13.2 **26-6S** (*C_1*, ^{1}A) 14.5

26-7S (*C_1*, ^{1}A) 14.5 **26-8S** (*C_1*, ^{1}A) 15.1 **26-9S** (*C_1*, ^{1}A) 18.6

26-10S (*C_1*, ^{1}A) 18.6 **26-11S** (*C_1*, ^{1}A) 20.4

Figure 9. Eleven optimized low-energy $(C_4F_8)_2Fe_2(CO)_6$ structures, with all fluorine atoms omitted for the sake of clarity.

The singly C_4F_8-bridged $(C_4F_8)_2Fe_2(CO)_6$ structures **26-1S**, **26-2S**, **26-3S**, **26-5S**, and **26-9S** can be derived from the singly C_4F_8-bridged $(C_4F_8)_2Fe_2(CO)_7$ structures **27-1S**, **27-4S**, **27-10S**, **27-6S**, and **27-15S**, respectively, by removing a terminal CO group. Thus, **26-1S**, **26-2S**, and **26-9S** all have a bridging perfluoro-1-methylpropylidene group, while **26-3S** and **26-5S** have a bridging perfluorobutylidene group and a bridging perfluoro-2-methylpropylidene group, respectively. Structures **26-1S**, **26-3S**, and **26-5S** all have terminal perfluoro-2-methylpropene groups, while **26-2S** and **26-9S** have a terminal perfluoro-2-butene group and a terminal perfluoro-1-butene group, respectively. Structure **26-1S** appears to be a favorable structure, since it lies 6.3 kcal/mol below the next lowest energy $(C_4F_8)_2Fe_2(CO)_6$ structure **26-2S**. Structures **26-3S**, **26-5S**, and **26-9S** lie at the even higher energies of 11.3, 13.2, and 18.6 kcal/mol above **26-1S**, respectively. The Fe–Fe distances of 2.59 to 2.63 Å in these five singly C_4F_8-bridged $Fe_2(\mu\text{-}C_4F_8)(C_4F_8)(CO)_6$ structures suggest formal Fe-Fe bonds. Thus, the iron of the $Fe(CO)_4$ group has the favored 18-electron configuration whereas the iron of the $Fe(C_4F_8)(CO)_2$ group has only a 16-electron configuration.

The triply C_4F_8- and CO-bridged $(C_4F_8)_2Fe_2(CO)_6$ structures **26-6S**, **26-7S**, **26-8S**, and **26-11S** can be derived from the triply C_4F_8- and CO-bridged $(C_4F_8)_2Fe_2(CO)_7$ structures **27-2S**, **27-9S**, **27-5S**, and **27-7S**, respectively, by removing a terminal CO group (Figure 9). Thus, **26-6S** has a bridging perfluoro-1-methylpropylidene group and a bridging perfluorobutylidene group whereas **26-7S** has two bridging perfluoro-1-methylpropylidene groups. Structure **26-8S** has a bridging perfluoro-1-methylpropylidene group and a bridging perfluoro-2-methylpropylidene group, while **27-11S** has two bridging perfluoro-2-methylpropylidene groups. Unlike the $Fe_2(\mu\text{-}C_4F_8)_2(\mu\text{-}CO)(CO)_6$ triply bridged structures, all of the $Fe_2(\mu\text{-}C_4F_8)_2(\mu\text{-}CO)(CO)_5$ triply bridged structures have much higher energies. Thus the relative energies of **26-6S**, **26-7S**, **26-8S**, and **26-11S** are 14.5, 14.5, 15.1, and 20.4 kcal/mol, respectively, above **26-1S**. The Fe–Fe distances of 2.45 to 2.50 Å in these four triply bridged $Fe_2(\mu\text{-}C_4F_8)_2(\mu\text{-}CO)(CO)_5$ structures suggest formal single Fe-Fe bonds, thereby giving one iron the favored 18-electron configuration and the other iron only a 16-electron configuration.

The singly CO-bridged $(C_4F_8)_2Fe_2(CO)_6$ structures **26-4S** and **26-10S** can be derived from the singly CO-bridged $(C_4F_8)_2Fe_2(CO)_7$ structures **27-3S** and **27-13S**, respectively, by removing a terminal CO group (Figure 9). Thus, **26-4S** has two terminal perfluoro-2-methylpropene ligands, whereas **26-10S** has one terminal perfluoro-2-methylpropene ligand and one perfluoro-2-butene ligand. Structures **26-4S** and **26-10S** lie 12.4 and 18.6 kcal/mol, respectively, in energy above **26-1S**. Again, interpreting the Fe–Fe distances of 2.782 and 2.687 Å in **26-4S** and **26-10S**, respectively, as formal single bonds gives one iron the favored 18-electron configuration but the other iron only a 16-electron configuration.

3.3 The Fe-Fe Wiberg bond indices given by natural bond orbital analysis

Wiberg bond indices (WBIs) for the iron-iron interactions in the optimized $(C_4F_8)_2Fe_2(CO)_n$ (n=7, 6) structures were determined using Weinhold's NBO analysis (Table 1). For metal-metal bonds involving d-block transition metals, the WBI values are only 10 to 30% of the formal bond order in singlet structures. For example, the WBI for the triply bridged formal Fe–Fe single bond in $Fe_2(CO)_9$ was found to be only 0.11.[38] The WBI values for the analogous formal Fe–Fe single bonds in the $(C_4F_8)_2Fe_2(CO)_n$ (n = 7, 6) structures were found to have similar values as $Fe_2(CO)_9$, ranging from 0.07 to 0.19. Generally, the WBI values are consistent with the bond orders assigned based on the iron-iron distances.

Table 1. The Wiberg bond indices (WBIs) of the Fe-Fe bonds by natural bond orbital (NBO) analysis for optimized low-lying $(C_4F_8)_2Fe_2(CO)_n$ (n=7, 6) structures.

Structure	Fe-Fe (Å)	Formal bond order	WBI (Fe-Fe)	Structure	Fe-Fe (Å)	Formal bond order	WBI (Fe-Fe)
27-1S	2.654	1	0.13	**27-18S**	2.837	1	0.10
27-2S	2.487	1	0.08	**27-19S**	2.604	1	0.08
27-3S	2.867	1	0.09	**27-20S**	2.658	1	0.08
27-4S	2.664	1	0.15	**27-21S**	2.686	1	0.14
27-5S	2.478	1	0.08	**27-22S**	2.681	1	0.13
27-6S	2.665	1	0.14	**27-23S**	2.658	1	0.08
27-7S	2.459	1	0.07	**26-1S**	2.597	1	0.19
27-8S	2.469	1	0.07	**26-2S**	2.628	1	0.18
27-9S	2.483	1	0.08	**26-3S**	2.600	1	0.17
27-10S	2.670	1	0.14	**26-4S**	2.782	1	0.12
27-11S	2.478	1	0.07	**26-5S**	2.593	1	0.17
27-12S	2.678	1	0.13	**26-6S**	2.472	1	0.09
27-13S	2.797	1	0.12	**26-7S**	2.499	1	0.09
27-14S	2.678	1	0.14	**26-8S**	2.446	1	0.10
27-15S	2.658	1	0.14	**26-9S**	2.599	1	0.19
27-16S	2.808	1	0.11	**26-10S**	2.687	1	0.13
27-17S	2.598	1	0.12	**26-11S**	2.452	1	0.09

3.4 ν(CO) vibrational frequencies

Table 2 lists the ν(CO) harmonic vibrational frequencies for the $(C_4F_8)_2Fe_2(CO)_n$ (n=7,6) and $C_4F_8Fe(CO)_4$ complexes obtained by the M06-L method. All of the terminal ν(CO) frequencies for $(C_4F_8)_2Fe_2(CO)_n$ (n = 7,6) and $C_4F_8Fe(CO)_4$ structures fall in the range from 2049 to 2193 cm^{-1}. The bridging ν(CO) frequencies are somewhat lower than the terminal ν(CO) frequencies, ranging from 1963 to 2047 cm^{-1}, which is typical for metal carbonyl derivatives. The highest bridging ν(CO) frequencies are for the semi-bridging CO groups in structures **26-7S**, **27-20S,** and **27-23S** with significantly different Fe–C distances to each of the iron atoms of the Fe_2 unit.

Table 2. The ν(CO) vibrational frequencies (in cm^{-1}) and infrared intensities (in km/mol, given in parentheses) of the optimized low-lying $(C_4F_8)_2Fe_2(CO)_n$ (n=7, 6) structures. Bridging ν(CO) frequencies are in *italics* whereas semibridging ν(CO) frequencies are in *underlined italics.*

Structure	ν(CO)
27-1S	2052(243), 2075(371), 2100(715), 2114(383), 2124(648), 2139(1341), 2172(138)
27-2S	*1990(396)*, 2104(35), 2108(869), 2114(205), 2121(1100), 2145(1582), 2171(18)
27-3S	*2009(443)*, 2071(182), 2079(125), 2106(715), 2113(950), 2133(574), 2172(191)
27-4S	2085(21), 2098(499), 2105(809), 2113(391), 2123(695), 2141(1254), 2176(93)
27-5S	*1986(372)*, 2101(124), 2107(792), 2111(385), 2123(905), 2144(1511), 2170(52)
27-6S	2084(2), 2093(584), 2104(379), 2111(712), 2115(869), 2135(1243), 2174(91)
27-7S	*1967(361)*, 2097(1), 2101(966), 2110(73), 2117(1287), 2140(1471), 2167(25)
27-8S	*1976(375)*, 2098(52), 2103(980), 2110(304), 2120(1064), 2142(1433), 2169(30)
27-9S	*2005(433)*, 2106(218), 2113(367), 2115(553), 2124(898), 2146(1648), 2172(41)
27-10S	2080(32), 2094(556), 2102(716), 2109(493), 2116(800), 2135(1193), 2173(98)
27-11S	*1981(394)*, 2100(2), 2104(1062), 2113(134), 2120(1231), 2144(1470), 2171(3)
27-12S	2079(49), 2095(633), 2104(399), 2112(206), 2114(1385), 2139(1064), 2176(81)
27-13S	*1969(408)*, 2077(39), 2088(215), 2103(905), 2118(770), 2137(645), 2172(107)
27-14S	2080(37), 2095(554), 2104(771), 2111(313), 2117(965), 2138(1139), 2175(77)
27-15S	2074(99), 2093(447), 2099(789), 2112(459), 2124(588), 2139(1348), 2174(103)
27-16S	*1973(424)*, 2082(38), 2086(90), 2109(954), 2114(862), 2140(629), 2174(105)
27-17S	2049(287), 2059(293), 2091(742), 2107(110), 2110(1151), 2132(1387), 2164(121)
27-18S	*1983(454)*, 2075(191), 2079(128), 2109(659), 2112(945), 2137(702), 2174(92)
27-19S	*1981(377)*, 2100(7), 2107(829), 2126(79), 2129(1102), 2153(1521), 2176(67)
27-20S	*2039(212)*, 2090(250), 2104(658), 2112(558), 2136(778), 2145(1165), 2178(255)
27-21S	2085(9), 2093(633), 2106(548), 2112(322), 2118(1261), 2139(1022), 2177(77)
27-22S	2080(46), 2094(653), 2105(472), 2110(283), 2116(1288), 2138(1050), 2176(84)
27-23S	*2030(254)*, 2093(277), 2106(644), 2115(544), 2136(700), 2146(1285), 2178(227)
26-1S	2071(105), 2093(756), 2109(737), 2111(562), 2128(1019), 2168(306)
26-2S	2059(150), 2095(747), 2105(796), 2110(314), 2119(1095), 2166(413)
26-3S	2066(145), 2091(755), 2109(517), 2113(946), 2126(917), 2170(230)
26-4S	*1976(469)*, 2072(42), 2081(299), 2098(1026), 2111(719), 2157(422)
26-5S	2066(130), 2090(656), 2108(614), 2112(951), 2126(941), 2168(249)
26-6S	*2012(396)*, 2082(646), 2109(572), 2115(1446), 2125(505), 2167(345)
26-7S	*2047(270)*, 2080(822), 2114(1326), 2120(491), 2135(482), 2174(410)
26-8S	*1997(407)*, 2085(586), 2107(596), 2118(1477), 2122(547), 2163(291)
26-9S	2069(109), 2092(769), 2107(763), 2109(479), 2122(1075), 2167(348)
26-10S	*1963(423)*, 2077(63), 2093(540), 2100(617), 2123(1140), 2162(76)
26-11S	*1970(409)*, 2085(585), 2097(576), 2111(1278), 2119(915), 2159(261)
14-1S	2087(837), 2112(997), 2115(403), 2176(236)
14-2S	2090(949), 2113(245), 2120(1083), 2179(197)
14-3S	2089(924), 2111(408), 2117(1000), 2178(172)
14-4S	2114(681), 2133(372), 2135(1019), 2193(152)
14-5S	2108(741), 2127(979), 2129(381), 2187(202)
14-6S	2105(777), 2123(590), 2127(843), 2185(184)
14-7S	2076(995), 2096(395), 2103(1109), 2165(255)
14-8S	2086(932), 2107(272), 2112(1060), 2172(316)
14-9S	2077(1001), 2097(401), 2104(1111), 2166(239)

4.Conclusions

The lowest energy $C_4F_8Fe(CO)_4$ structure is not the very stable experimentally known ferracyclopentane isomer $(CF_2CF_2CF_2CF_2)Fe(CO)_4$ obtained from $Fe(CO)_{12}$ and tetrafluoroethylene. Instead isomeric (perfluoroolefin)$Fe(CO)_4$ structures derived from perfluoro-2-butene, perfluoro-1-butene, and perfluoro-2-methylpropene are significantly lower energy structures by up to ~17 kcal/mol. However, the activation energies for the required fluorine shifts from one carbon to an adjacent carbon atom to form these (perfluoroolefin)$Fe(CO)_4$ complexes are very high (e.g., ~70 kcal/mol). Therefore the ferracyclopentane isomer $(CF_2CF_2CF_2CF_2)Fe(CO)_4$, which does not require a fluorine shift to form from $Fe_3(CO)_{12}$ and tetrafluoroethylene, is the kinetically favored product.

Perfluorocarbene ligands, which do not appear in the lowest energy structures of the mononuclear $C_4F_8Fe(CO)_4$ system, appear as bridging ligands in the lowest energy structures of the binuclear $(C_4F_8)_2Fe_2(CO)_n$(n = 7, 6) derivatives. The terminal C_4F_8 ligands in the lowest energy $(C_4F_8)_2Fe_2(CO)_n$ structures are perfluoroolefins.

Acknowledgements

Guoliang Li thanks the University of Georgia for a visiting professorship during 2014-2015. The research at the University of Georgia was supported by the U.S. National Science Foundation Grant CHE-1661604.

The authors declare no competing financial interests.

Supporting Information

Table S1. Comparison of total energies and relative energies for various optimized low-lying structures of the $C_4F_8Fe(CO)_4$ complexes using four different methods: M06-L, B3LYP, BP86, and BPW91. Table S2: Total energies, relative energies, ZPE-corrected total energies and ZPE-corrected relative energies for optimized low-energy structures of the $(C_4F_8)_2Fe_2(CO)_n$ (n=7, 6) and $C_4F_8Fe(CO)_4$ complexes at the M06-L/cc-pVTZ level; Table S3: Vibrational frequencies and infrared intensities for optimized low-energy structures of the $(C_4F_8)_2Fe_2(CO)_n$ (n=7, 6) and $C_4F_8Fe(CO)_4$ complexes at the M06-L/cc-pVTZ level; Table S4: Cartesian coordinates for optimized low-energy structures of the $(C_4F_8)_2Fe_2(CO)_n$(n=7, 6) and $C_4F_8Fe(CO)_4$ complexes at the M06-L/cc-pVTZ level; Complete Gaussian 09 reference.

Literature References

[1] W. R. McClellan, Perfluoroalkyl and perfluoroacyl metal carbonyls, *J. Am. Chem. Soc.*, 1961, **83**, 1598-1600.

[2] W. Hieber, W. Beck, and E. Lindner, Trifluoracetyl- und Trifluormethyl-metall-carbonyle, *Z. Naturforsch.*, 1961, **16b**, 229-231.

[3] F. Calderazzo, in Encyclopedia of Inorganic Chemistry, 2nd Edition, ed. R. B. King, , Wiley, Chichester, 2005, pp.764.

[4] R. P. Hughes, Fluorine as a ligand substituent in organometallic chemistry. A second chance and a second research career, *J. Fluor. Chem.*, 2010, **131**, 1059-1070.

[5] M. F. Kuehnel and D. Lentz, Fluorinated dienes in transition-metal chemistry—the rich chemistry of electron-poor ligands, *Dalton Trans.*, 2010, **39**, 9745-9759.

[6] D. J. Harrison, G. M. Lee, M. C. Leclerc, I. Korobkov, and R. T. Baker, Cobalt fluorocarbenes: cycloaddition reactions with tetrafluoroethylene and reactivity of the perfluorometallacyclic products, *J. Am. Chem. Soc.*, 2013, **135**, 18296-18299.

[7] J. L. Kiplinger, T. G. Richmond and C. E. Osterberg, Activation of carbon-fluorine bonds by metal-complexes, *Chem. Rev.*, 1994, **94**, 373-431.

[8] B. L. Booth, R. N. Haszeldine, P. R. Mitchell and J. J. Cox, Reactions of fluoro-olefins with octacarbonyldicobalt, *Chem. Commun.*, 1967, **117**, 529-530.

[9] B. L. Booth, R. N. Haszeldine, P. R. Mitchell and J. J. Cox, Metal carbonyl chemistry. Part V. Reactions of fluoro-olefins with octacarbonyldicobalt, *J. Chem. Soc. A.*, 1969, 691-698.

[10] K. F. Watterson and G. Wilkinson, Perfluorolefin transition metal complexes, *Chem. & Ind.*, 1959, 991-991.

[11] K. F. Watterson and G. Wilkinson, Fluorocarbon transition metal complexes, *Chem. & Ind.*, 1960, 1358-1358.

[12] H. H. Hoehn, L. Pratt, K. F. Watterson and G. Wilkinson, Transition-metal fluorocarbon complexes. Part I. Derivatives of perfluoro-olefins, *J. Chem. Soc.*, 1961, 2738-2745.

[13] N. A. Richardson, Y. Xie, B. B. King and H. F. Schaefer, Flat potential energy surface of the saturated binuclear homoleptic chromium carbonyl $Cr_2(CO)_{11}$ with one, two, and three bridging carbonyls: comparison with the well-known $[HCr_2(CO)_{10}]^-$ anion and the related $[(\mu\text{-H})_2Cr_2(CO)_9]^{2-}$ and $[(\mu\text{-H})_2Cr_2(CO)_8]^{2-}$ dianions, *J. Phys. Chem. A.*, 2001, **105**, 11134-11143.

[14] S. Li, N. A. Richardson, Y. Xie, B. B. King and H. F. Schaefer, The rule breaking

$Cr_2(CO)_{10}$. A 17 electron Cr system or a Cr=Cr double bond? *Faraday Discuss.*, 2003, **124**, 315-329.

[15] T. Ziegler and J. Autschbach, Theoretical methods of potential use for studies of inorganic reaction mechanisms, *Chem. Rev.*, 2005, **105**, 2695-2722.

[16] M. Bühl and H. Kabrede, Geometries of transition-metal complexes from density-functional theory, *J. Chem. Theory Comput.*, 2006, **2**, 1282-1290.

[17] M. Brynda, L. Gagliardi, P. O. Widmark, P. P. Power and B. O. Roos, A quantum chemical study of the quintuple bond between two chromium centers in [PhCrCrPh]: trans-bent versus linear geometry, *Angew. Chem. Int. Ed.*, 2006, **45**, 3804-3807.

[18] N. Sieffert and M. Bühl, Hydrogen generation from alcohols catalyzed by ruthenium-triphenylphosphine complexes: multiple reaction pathways, *J. Am. Chem. Soc.*, 2010, **132**, 8056-8070.

[19] P. Schyman, W. Lai, H. Chen, Y. Wang and S. Shaik, The directive of the protein: how does cytochrome P450 select the mechanism of dopamine formation? *J. Am. Chem. Soc.*, 2011, **133**, 7977-7984.

[20] R. D. Adams, W. C. Pearl, Y. O. Wong, Q. Zhang, M. B and Hall, J. R, Tetrarhena-heterocycle from the palladium-catalyzed dimerization of $Re_2(CO)_8(\mu\text{-}SbPh_2)(\mu\text{-}H)$ exhibits an unusual host–guest behavior, *J. Am. Chem. Soc.*, 2011, **133**, 12994-12997.

[21] R. R. Lonsdale, J. Olah, A. J. Mulholl and J. N. Harvey, Does compound I vary significantly between isoforms of cytochrome P450? *J. Am. Chem. Soc.*, 2011, **133**, 15464-15474.

[22] Y. Zhao and D. G. Truhlar, A new local density functional for main-group thermochemistry, transition metal bonding, thermochemical kinetics, and noncovalent interactions, *J. Chem. Phys.*, 2006, **125**, 194101-194107.

[23] Y. Zhao and D. G. Truhlar, The M06 suite of density functionals for main group thermochemistry, thermochemical kinetics, noncovalent interactions, excited states, and transition elements: two new functionals and systematic testing of four M06-class functionals and 12 other functionals, *Theor. Chem. Acc.*, 2008, **120**, 215-241.

[24] Y. Zhao and D. G. Truhlar, Density functionals with broad applicability in chemistry, *Acc. Chem. Res.*, 2008, **41**, 157-167.

[25] T. H. Dunning, Gaussian basis sets for use in correlated molecular calculations. I. The atoms boron through neon and hydrogen, *J. Chem. Phys.*, 1989, **90**, 1007-

1023.

[26] N. B. Balabanov and K. A. Peterson, Systematically convergent basis sets for transition metals. I. All-electron correlation consistent basis sets for the 3d elements Sc–Zn, *J. Chem. Phys*., 2005, **123**, 064107-064115.

[27] A. D. Becke, Density-functional thermochemistry. III. The role of exact exchange, *J. Chem. Phys.* 1993, **98**, 5648-5652.

[28] C. Lee, W. Yang, and R. G. Parr, Development of the Colle-Salvetti correlation-energy formula into a functional of the electron density, *Phys. Rev. B* 1988, **37**, 785-789.

[29] A. D. Becke, Density-functional exchange-energy approximation with correct asymptotic behavior, *Phys. Rev. A* 1988, **38**, 3098-3100.

[30] J. P. Perdew, Density-functional approximation for the correlation energy of the inhomogeneous electron gas, *Phys. Rev. B* 1986, **33**, 8822-8824.

[31] J. P. Perdew and Y. Wang, Accurate and simple analytic representation of the electron-gas correlation energy, *Phys. Rev. B* 1992, **45**, 13244-13249.

[32] G. L. Gutsev, and C. W. Bauschlicher, Electron affinities, ionization energies, and fragmentation energies of Fe_n Clusters (n = 2−6): A Density functional theory study, J. Phys. Chem. A, 2003, **107**, 7013-7023.

[33] P. Limon, A. Miralrio, M. Castro, Adsorption and dissociation of carbon monoxide on iron and iron-carbon clusters: Fe_n + 2CO and Fe_nC + 2CO, n = 4 and 7. A theoretical study, Comp. Theor. Chem., 2018, **1129**, 37-47.

[34] M. J. Frisch, et al, Gaussian 09, Revision B.01; Gaussian, Inc.; Wallingford CT, 2010 (see Supporting Information for details).

[35] H. P. Hratchian and H. B. Schlegel, Accurate reaction paths using a Hessian based predictor-corrector integrator, *J. Chem. Phys.* 2004, **120**, 9918-9924.

[36] H. P. Hratchian and H. B. Schlegel in *Theory and Applications of Computational Chemistry: The First 40 Years*; C. E. Dykstra, G. Frenking, K. S. Kim and G. Scuseria, Eds.; Elsevier: Amsterdam, The Netherlands, 2005.

[37] H. P. Hratchian and H. B. Schlegel, Using Hessian updating to increase the efficiency of a Hessian based predictor-corrector reaction path following method, *J. Chem. Theory Comput.* 2005, **1**, 61-69.

[38] H. Wang, Y. Xie, R. B. King and H. F. Schaefer, Remarkable aspects of unsaturation in trinuclear metal carbonyl clusters: the triiron species $Fe_3(CO)_n$ (n = 12, 11, 10, 9), *J. Chem. Soc*., 2006, **128**, 11376-11384.